Catalytic Control and Coupling Efficiency of the *Escherichia coli* F_oF_1 ATP Synthase: Influence of the F_o Sector and ϵ Subunit on the Catalytic Transition State†

Yelena B. Peskova and Robert K. Nakamoto*

Department of Molecular Physiology and Biological Physics, University of Virginia, P.O. Box 800736, Charlottesville, Virginia 22908-0736

Received June 15, 2000; Revised Manuscript Received July 17, 2000

ABSTRACT: The rate-limiting transition state of steady-state ATP hydrolysis and synthesis reactions in the F_oF_1 ATP synthase involves the rotation of the γ, ϵ, and c subunits. To probe the role of the transport and coupling mechanisms in controlling catalysis, kinetic and thermodynamic parameters of ATP hydrolysis were determined for enzymes in the presence of the detergent lauryldimethylamine oxide (LDAO), which uncouples active transport and disables the inhibitory effect of the ϵ subunit. At 5 mM LDAO or greater, the inhibitory effects of ϵ subunit are abrogated in both purified F_1 and membranous F_oF_1. In these conditions, LDAO solubilized F_oF_1 has a higher k_{cat} for ATP hydrolysis than F_1. These results indicate an influence of F_o on F_1 even though catalysis is uncoupled from transport. The $\alpha_3\beta_3\gamma$ complex free of the ϵ subunit is activated at a lower concentration of 0.5 mM LDAO. Significantly, the γY205C mutant enzyme is similarly activated at 0.5 mM LDAO, suggesting that the mutant enzyme lacks ϵ inhibition. The γY205C F_oF_1, which has a k_{cat} for ATP hydrolysis 2-fold higher than wild type, has an ATP synthesis rate 3-fold lower than wild type, showing that coupling is inefficient. Arrhenius and isokinetic analyses indicate that enzymes that are free of ϵ subunit inhibition have a different transition-state structure from those under the influence of the ϵ subunit. We propose that the ϵ subunit is one of the factors that determines the proper transition-state structure, which is essential for efficient coupling.

Coupled transport in the F_oF_1 ATP synthase involves rotation of the γ (*1*−*3*) and ϵ (*4*−*6*) subunits and the ring of 10−12 c subunits (*7*, *8*; for reviews see refs *9*−*13*). In the catalytic domain, steady-state ATP hydrolysis or synthesis involves the rotation of the γ subunit relative to the $\alpha_3\beta_3$ complex (see refs *10* and *13*−*15* for discussions). Steady-state catalysis, which involves participation of all three catalytic sites, is concomitant with rotation because rotation is blocked by inhibitors of cooperative steady-state ATP hydrolysis (*1*−*3*), and steady-state hydrolysis is blocked by chemical cross-linking of γ or ϵ (rotor) and β (stator) subunits (*16*, *17*). The transport mechanism in the F_o sector is not well understood, but models also employ a rotational movement of the c subunit oligomer relative to the a subunit (*18*−*20*). Importantly, inhibition of transport attenuates rotation of the γ subunit in the catalytic domain (*4*, *6*, *7*, *21*). It is reasonable that the transport and catalytic mechanisms are coupled by the rotor subunits. Recent results from several laboratories (*22*−*29*) have demonstrated that the $b_2\delta$ peripheral stem fixes the stator elements, a and $\alpha_3\beta_3$, together.

Mutagenic, kinetic, and thermodynamic approaches have shown that several amino acids in the *Escherichia coli* F_oF_1 are involved in intersubunit, rotor−stator interactions important for the mechanisms of transport and catalysis, and the efficient coupling between them. Substitution of these amino acids perturbs rotor−stator interactions occurring between the γ and β subunits (*14*, *30*−*33*) and the a and c subunits (*34*−*36*). The altered interactions have been shown to affect the rate-limiting transition state of steady-state catalysis of ATP hydrolysis and synthesis (*31*, *33*, *36*). Because steady-state catalysis is concomitant with rotation, the rate-limiting step of catalysis involves rotation of the γ subunit (*13*, *14*). Interactions among the rotor subunits, γ, ϵ and c, also influence catalysis (*37*−*48*). Association of F_1 with the transport F_o sector results in activation of the enzyme (*31*), while ϵ subunit association with the $\alpha_3\beta_3\gamma$ catalytic domain inhibits ATP hydrolysis rates (*49*, *50*). Perturbations in each of these intersubunit interactions affect the rate-limiting transition state and coupling efficiency, which suggests that the catalytic transition state and coupling are interrelated.

A critical region for the coupling mechanism resides at the interface between the γ and ϵ subunits, and the F_o, probably with the c subunits. This region has been structurally defined by cross-linking studies that have implicated at least γTyr205, γTyr207, several ϵ subunit residues, and the polar loop of the *c* subunits (*39*, *42*−*44*, *47*, *48*). Furthermore, genetic studies established that these interactions play a role in coupling. Uncoupling mutations in this region have been characterized and intergenic second-site mutations suppressed their deleterious effects (*40*, *46*). In addition, a cross-link between γY207C and *c*Q42C causes reduced coupling (*48*).

† This work was supported by U.S. Public Health Service Grant GM50957.

* To whom correspondence should be addressed: Tel 804-982-0279; fax 804-982-1616; e-mail rkn3c@virginia.edu.

10.1021/bi0013694 CCC: $19.00
Published on Web 08/25/2000

Taken together, these results define regions in each of the three subunits that interact to maintain efficient coupling. This region, which is not in physical contact with the α and β subunits, is partially modeled into the recent crystallographic structure of the yeast F_oF_1 complex (*12*). The structure suggests that the coupling domain modulates catalysis through indirect conformational effects via the γ subunit. Cross-linking studies suggest direct interactions between ϵ subunit and the α and β subunits and these interactions may also participate in coupling (*6*, *16*, *51*, *52*).

Here, we assess the influence of transport and coupling on the catalytic mechanism. Lötscher et al. (*53*) and Dunn et al. (*54*) previously showed that the detergent lauryldimethylamine oxide (LDAO)[1] releases the F_1 complex from the inhibitory effects of the ϵ subunit, even though ϵ subunit remains associated with the complex. Similarly, replacement of γTyr205 with cysteine causes a 3.5-fold increase in steady-state hydrolytic activity of F_1 (*44*) and may provide a mutant form in which the ϵ subunit inhibition is abrogated. We take advantage of these properties to characterize the influence of the transport F_o sector and the $\gamma-\epsilon-$c interface on steady-state catalysis. The kinetic and thermodynamic analyses establish that the $\gamma-\epsilon-$c interface plays a role in determining the transition-state structure of the rotational catalytic mechanism and that the proper transition state is critical in achieving maximal coupling efficiency.

EXPERIMENTAL PROCEDURES

Strains and Plasmids. Wild-type and mutant forms of F_oF_1 ATP synthase were expressed from plasmid-borne *unc* operon on pACWU1.2 (*55*) in strain DK8 (*bglR thi-1 rel-1 HfrPO1* Δ(*uncB*−*uncC*) *ilv::Tn10*; *56*). Construction of variants of pACWU1.2 carrying the mutations γE208K (*46*) and aG213N+aL251V (*36*), with or without the amino-terminal β-FLAG affinity tag (*55*), was previously described. The γM23K mutation from pBWU13.4 (*33*) was isolated on the *Kpn*I−*Spe*I restriction fragment and ligated into pACWU1.2. The γY205C mutation was introduced by oligonucleotide-directed mutagenesis. Plasmid pBγKS (*55*) was the template for the mutagenesis reactions to introduce γY205C by polymerase chain reaction (*57*) with the *Pfu* thermophilic polymerase (Stratagene, La Jolla, CA) with primers 5′-AAATCCTGGGATtgcCTGTACGAAC-3′ (sense strand; cysteine codon in lowercase letters) and 5′-GTTCG-TACAGgcaATCCCAGGATTT-3′ (antisense strand). After sequencing of the entire insert, the *Kpn*I−*Spe*I fragment was ligated into pACWU1.2 containing the β-FLAG tag.

Molecular biology procedures were performed according to manufacturers' instructions or as detailed by Sambrook et al. (*58*). Restriction and DNA-modifying enzymes were obtained from Roche Molecular Biochemicals (Indianapolis, IN), Gibco−BRL (Rockville, MD), or New England Biolabs (Beverly, MA).

Enzyme Preparations. To prepare F_oF_1-containing membrane vesicles, strains were grown until mid-log phase in minimal medium containing 1.1% glucose at 37 °C, and membranes were isolated as previously described (*59*). Protein concentrations were determined by the method of Lowry et al. (*60*). The membrane vesicles were finally suspended at 20−40 mg/mL in a buffer consisting of 5 mM Tris-HCl, 70 mM KCl, 0.5 mM DTT, and 55% glycerol at pH 8.0.

Purification of FLAG-F_1 was performed as previously described (*46*). ϵ subunit was purified from wild-type F_1 by the method of Smith and Sternweis (*61*).

Determination of F_1 content in membrane preparations was performed by a quantitative immunoblot assay described previously (*31*). Purified F_1 was used as a reference standard.

Enzymatic Assays. Formation of an electrochemical gradient of protons was followed by use of acridine orange at pH 7.5 as previously described (*62*). ATP hydrolysis rates were determined as previously described (*14*) at 30 °C by addition of 0.1−0.3 mg/mL membrane protein or 0.5 or 26 nM purified F_1 to a buffer containing 50 mM HEPES−KOH, 10 mM ATP, 5 mM $MgSO_4$, and 1 μM carbonyl cyanide *m*-chlorophenylhydrazone (CCCP), pH 7.5, with 5 mM phosphoenolpyruvate, 50 μg/mL pyruvate kinase, and 0−22 mM LDAO as specified. Four time points were taken and the amount of P_i generated was determined as previously described (*63*). P_i production was required to be linear over time. If the rate fell during the course of the assay, the enzyme was considered unstable in those conditions. In the case of the Arrhenius analysis, the pH was adjusted to 7.5 at the appropriate temperature (*31*). ATP synthesis rates were determined as previously described (*14*) at 30 °C. The concentration of free Mg^{2+} and Mg·ATP was calculated with the algorithm of Fabiato and Fabiato (*64*).

Materials. ATP, LDAO, NADH, and acridine orange were obtained from Sigma Chemical Co. (St. Louis, MO), and pyruvate kinase was from Roche Molecular Biochemicals. Venturicidin A was obtained from Dr. Bernhard Liebermann at the Institut für Pharmazie, Friedrick-Schiller Universität, Germany. All other reagents were of the highest grade and purity available.

RESULTS

Activation of ATP Hydrolytic Activity by LDAO. Steady-state ATP hydrolytic rates of *E. coli* F_oF_1 in membranes or purified F_1 were determined in V_{max} conditions at pH 7.5 in the presence of 10 mM ATP and 5 mM $MgSO_4$ at 30 °C. A strong ADP trap or ATP-regenerating system was always present to avoid possible complications from ADP·Mg inhibition (*65*). LDAO activated steady-state hydrolysis of membranous F_oF_1 to a turnover of 890 s^{-1} with 10 mM LDAO, which was an approximately 3-fold increase over enzyme without LDAO (Figure 1A). Similarly, purified F_1 was activated to 510 s^{-1}, an almost 4-fold increase. The activations occurred over a similar range of LDAO concentrations and were in agreement with those reported by Lötscher et al. (*53*) and Dunn et al. (*54*). Because F_oF_1 is activated over a similar LDAO concentration range as F_1, the results indicate that F_oF_1 is also ϵ-inhibited and the inhibition is disabled by LDAO. This interpretation is consistent with the findings of Schulenberg and Capaldi (*66*) and Kato-Yamada et al. (*67*). Previously, we and others (*31*, *46*, *68*) suggested that ϵ-inhibition of F_1 was released upon binding to F_o because the turnover of ATP hydrolysis by F_1 was increased approximately 4-fold upon binding to F_o (see below).

[1] Abbreviations: CCCP, carbonyl cyanide *m*-chlorophenylhydrazone; LDAO, lauryldimethylamine oxide.

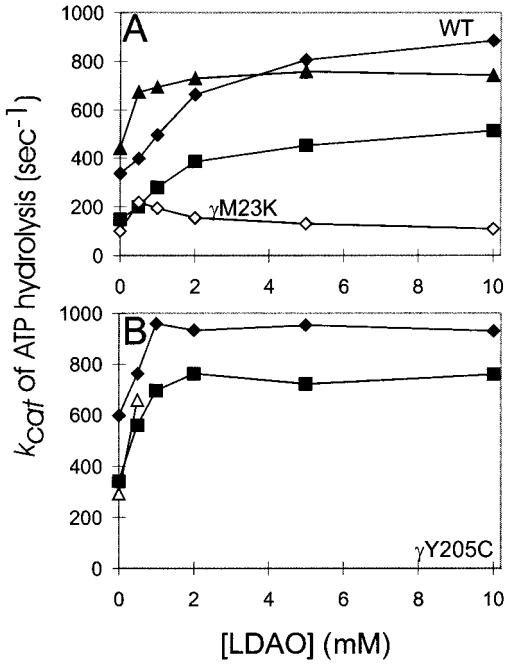

FIGURE 1: k_{cat} at 30 °C for ATP hydrolysis as a function of LDAO concentration. ATP hydrolytic activities were determined in the presence of 0−22 mM LDAO as described under Experimental Procedures. The enzyme preparations were as follows: (◆) F_oF_1 enzyme in membrane vesicles; (■) F_1 enzyme at a concentration of 26 nM; (▲), F_1 dissociated from ϵ subunit by dilution (F_1 concentration was 0.5 nM; the K_D for ϵ to the $\alpha_3\beta_3\gamma$ complex ∼ 3 nM; *31*, *37*, *68*). (A) Wild type is shown by the solid symbols and γM23K F_oF_1 by (◇). (B) γY205C enzymes. The diluted γY205C enzyme (△) was unstable in 1 mM LDAO or greater. The rates of hydrolysis decreased during the time course of the measurements and could not be determined. This was also the case for γM23K F_1 in LDAO.

Lötscher et al. (*53*) and Dunn et al. (*54*) reported that ϵ subunit remains associated with F_1 complex even in the presence of 9 mM LDAO, a concentration that completely eliminated ϵ inhibition. Furthermore, loss of inhibition did not involve the δ subunit because LDAO activation of F_1 was independent of this subunit (*53*). To test the effect of LDAO on F_1 in the absence of ϵ subunit, purified F_1 was diluted to 0.5 nM, a concentration below the K_D for ϵ subunit, which is ∼3 nM (*31*, *37*, *68*). In the ϵ-dissociated form, the enzyme was also activated by LDAO but at a much lower concentration (<0.5 mM versus 1−2 mM; Figure 1A). Thus, there is a pronounced effect by the detergent on the minimal catalytic complex $\alpha_3\beta_3\gamma$, an effect that is different from ϵ inhibition. This observation is also consistent with previous results for activation of ϵ-depleted F_1 by LDAO (*54*).

Significantly, association of F_1 with F_o stimulated even higher catalytic turnover. With increasing concentrations of LDAO and the release of ϵ inhibition, the hydrolytic turnover of membranous F_oF_1 was at least 70% higher than for F_1 alone and slightly higher than the LDAO-activated $\alpha_3\beta_3\gamma$ complex (Figure 1). This activation remained even in the presence of up to 22 mM LDAO and occurred at concentrations much greater than that required to uncouple the transport mechanism from catalysis.

Coupling in this case was assessed by the inhibition of ATP hydrolytic activity by either the transport inhibitor, venturicidin (*69*, *70*), or a double subunit a mutation, aG213N+aL251V (*36*), both of which attenuate the transport mechanism (compare the k_{cat} of enzymes at 0 LDAO). This indirect attenuation on catalysis was eliminated with as little as 0.4 mM LDAO (Figure 2). At higher LDAO, the activation of the mutant enzyme was nearly identical to the wild-type enzyme with or without venturicidin.

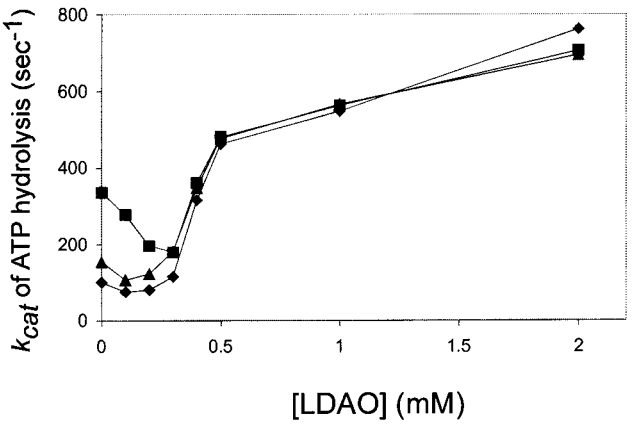

FIGURE 2: LDAO-dependent uncoupling: Effect of LDAO on the aG213N + aV251L mutant membranous F_oF_1 (*36*) (▲), on wild-type F_oF_1 inhibited by 5 μg/mL venturicidin (◆), and, for comparison, on wild-type F_oF_1 without inhibitors (■).

Similar to that observed by Lötscher et al. (*53*), the presence of less than 0.4 mM LDAO caused inhibition of wild-type F_oF_1 activity (Figure 2). This effect appears to be due to the F_o sector because purified F_1 activity is not inhibited at low LDAO concentrations (data not shown). This inhibition is likely caused by disruption of the membranous F_o structure, which creates a similar attenuation of catalytic activity as venturicidin or the F_o aG213N+aL251V mutation. We note that the aG213N+aL251V F_oF_1 enzyme does not have altered unisite catalytic parameters indicating that the effect of transport is only on steady-state rotational catalysis.[2]

The above results show that the presence of F_o stimulated a higher turnover than that for F_1 even though LDAO caused the loss of functional coupling between transport and catalysis. We note, however, that it was not possible to demonstrate directly whether the F_oF_1 complex was still intact. Efforts to assay the association of F_o with F_1 in high concentrations of LDAO by sucrose density gradient centrifugation gave only ambiguous results (data not shown). In light of these technical difficulties, we must assume that, because of the obvious difference between the behavior of the F_1 and F_oF_1 complexes, at least some portion of F_o must remain associated with F_1.

Effects of LDAO on γM23K and γE208K Mutant Enzymes. We previously showed that the γM23K mutation alters interactions between γ and β subunits (*14*, *31*, *32*). γM23K F_1 has the same inhibition constant for ϵ subunit as wild type (*31*); however, the LDAO activation of the mutant enzyme is partially blocked (Figure 1A). Turnover of the γM23K F_oF_1 is activated 2-fold at 0.5 mM LDAO but is not further increased at higher LDAO concentrations. These data indicate that the γM23K mutation prevents the LDAO activation and suggest that the perturbation caused by LDAO cannot overcome the increased energy of interaction between γ and β subunit caused by the mutation (*31*). Purified γM23K F_1 is unstable in LDAO and activity disappears with time.

[2] Y. B. Peskova and R. K. Nakamoto, manuscript in preparation.

Table 1: Kinetic Parameters for γY205C Mutant versus Wild-Type Enzymes at 30 °C[a]

preparation	ATP synthesis[b] (s^{-1})	ATP hydrolysis (s^{-1})	ATP synthesis/ ATP hydrolysis[c]
WT F_oF_1	25	336	0.074
γY205C F_oF_1	8.0	599	0.013
WT F_1 ($+\epsilon$)		149[d]	
γY205C F_1 ($+\epsilon$)		346[d]	
γY205C F_1 + 20 nM ϵ		292[e]	
WT F_1 dilute ($-\epsilon$)		440[f]	
γY205C F_1 dilute ($-\epsilon$)		297[f]	

[a] All values reported are the averages of at least three trials. [b] NADH-driven ATP synthesis was measured at 30 °C as previously described (*14*). [c] The ATP synthesis/ATP hydrolysis ratio is the k_{cat} of ATP synthesis divided by the k_{cat} of ATP hydrolysis determined for F_oF_1 enzyme in membrane vesicles at 30 °C. [d] The concentration of F_1 in the assay was 26 nM. [e] The concentration of F_1 in the assay was 26 nM plus 20 nM additional purified ϵ subunit. [f] The concentration of F_1 in the assay was 0.5 nM.

We also assessed the effect of LDAO on the γE208K mutant enzyme. This mutation, which is in the $\gamma-\epsilon-$c interface, causes inefficient coupling between transport and catalysis and reduced steady-state catalytic rates (*46*). In contrast to γM23K, the γE208K mutant enzyme was activated by LDAO very similar to wild type; however, the k_{cat} of the γE208K enzyme was always about half of the equivalent wild-type form (F_oF_1, F_1, or ϵ-free F_1) and at all LDAO concentrations up to 10 mM (data not shown). Clearly, the γE208K amino acid substitution influences catalytic turnover even though its location is distant from the catalytic domain (*12*, *71*). The effects of the γE208K mutation indicate the importance of the $\gamma-\epsilon-$c interface in controlling catalysis.

The γY205C Substitution Abrogates the Effects of ϵ Subunit. In contrast to γE208K, the nearby γY205C mutant enzyme behaved quite differently and as though the ϵ inhibition was abrogated (compare Figure 1 panels A and B). The mutant enzyme, in membranes or F_1 alone, had a higher k_{cat} for ATP hydrolysis (Table 1). Addition of excess ϵ subunit to γY205C F_1 had only a small effect on activity, which indicated that the γY205C F_1 still had ϵ subunit bound and that the lack of inhibition was not due to a lower affinity of ϵ subunit for F_1 complex. Moreover, dilution of the mutant F_1 to dissociate ϵ subunit did not result in activation of the enzyme, suggesting that the already high k_{cat} of the mutant F_1 was not subject to ϵ inhibition.

The γY205C F_1 and F_oF_1 response to LDAO was very similar to wild type, ϵ-free F_1, with the mutant F_oF_1 having higher turnover rates (Figure 1B). These results suggested that the mutant γY205C enzyme complexes were already free of ϵ inhibition. The diluted γY205C F_1 (to release ϵ subunit) became unstable at greater than 1 mM LDAO.

In addition to higher turnover, the γY205C substitution also caused less efficient coupling. The k_{cat} for NADH-driven ATP synthesis was significantly lower than wild type even though the k_{cat} for ATP hydrolysis was much higher (Table 1). Control experiments were done with acridine orange fluorescence to determine the extent of NADH proton pumping (see Experimental Procedures). These experiments showed that the mutant membranes achieved a similar extent of NADH-driven electrochemical gradient of protons as the wild-type membranes (data not shown). If the ATP hydrolytic activity represents the catalytic competency of the enzyme, then the ratio of ATP synthesis to hydrolysis is an indicator of coupling efficiency (*31*). The ratio for the mutant enzyme is almost 6-fold lower for the mutant enzyme complex (Table 1).

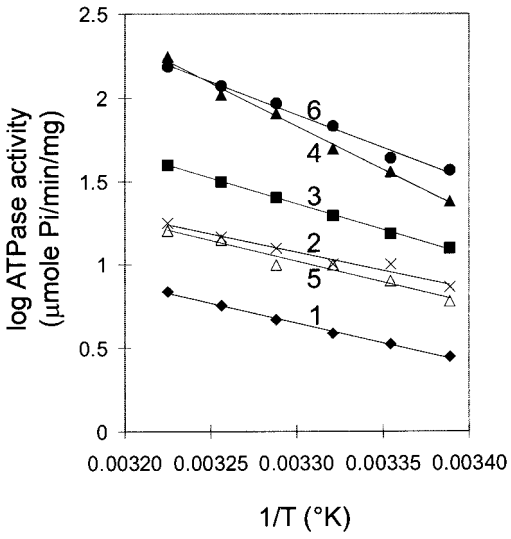

FIGURE 3: Effect of LDAO on F_oF_1 and F_1 Arrhenius plots. ATPase activities were determined as described under Experimental Procedures between 22 and 37 °C. All enzymes shown here are wild type with F_oF_1 in native membrane vesicles or F_1 purified as previously described (*46*). The data are from the following preparations: 1, F_oF_1 in membranes (◆); 2, F_oF_1 plus 10 mM LDAO (×); 3, 26 nM F_1 (■); 4, 0.5 nM F_1 (▲); 5, 0.5 nM F_1 plus 20 nM added ϵ subunit (△); and 6, 26 nM F_1 plus 10 mM LDAO (●). The data are plotted as specific activity for clarity. The lines are linear regression fits over the temperature range of each preparation.

Effect of ϵ Subunit on the Transition State. To provide information on the effect of LDAO and the ϵ subunit on the rate-limiting step of ATP hydrolysis, we determined the thermodynamic parameters of the steady-state transition state (*14*). The Arrhenius plot of LDAO-treated or ϵ-free enzymes from 22 to 37 °C had different slopes compared to ϵ-replete enzymes (Figure 3). We note that the ATP hydrolytic rates remained constant over time at all temperatures, indicating that the enzymes were stable in the assay conditions. Furthermore, each Arrhenius plot remained linear, indicating that the rate-limiting step did not change over the temperature range for a given LDAO concentration. Calculation of the thermodynamic parameters of the steady-state transition state showed that elimination of the ϵ subunit inhibition on F_1 [by diluting the enzyme to 0.5 nM to dissociate ϵ subunit (Figure 3, line 4) or by adding 10 mM LDAO, (Figure 3, lines 2 and 6)] resulted in a significantly higher E_A. Although these data are difficult to interpret because of the multiple effects of LDAO on the enzyme, the results suggest that ϵ has an effect on the steady-state transition state.

We assessed the effects of the ϵ subunit on the transition state by isokinetic analysis. Previously we have shown that the thermodynamic properties of the F_oF_1 and F_1 steady-state transition state from a variety of sources or carrying different mutations conform to a linear relationship (Figure 4A; *14*, *31*, *36*). This linear isokinetic relationship indicates that each of the enzymes utilizes the same transition-state structure at the rate-limiting step. The position along the line indicates differences in the number of bonds between the substrates and enzyme or within the enzyme that must be

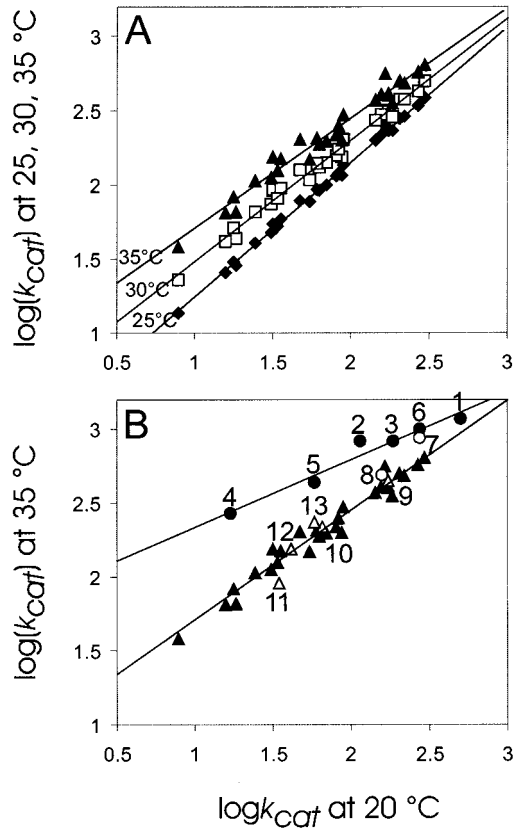

FIGURE 4: Isokinetic correlations of various F_oF_1 and F_1 enzymes carrying different amino acid substitutions or from different sources: enzymes without the influence of ϵ subunit have a different linear relationship. (A) Log k_{cat} at 20 °C versus log k_{cat} at 25 (◆), 30 (□), and 35 °C (▲). See refs *14*, *31*, and *80* for a list of the enzymes included in the plot. (B) Isokinetic correlation of enzymes without ϵ, treated with LDAO or carrying the γY205C substitution. Only the 20 °C versus 35 °C comparison is shown for clarity. (●): 1, wild-type F_oF_1 in 10 mM LDAO; 2, wild-type F_1 at 0.5 nM (diluted); 3, wild-type F_1 at 26 nM in 10 mM LDAO; 4, γM23K F_oF_1 in 10 mM LDAO; 5, γM23K F_1 at 0.5 nM (diluted); 6, γE208K F_oF_1 in 10 mM LDAO. (○): 7, γY205C F_oF_1; 8, γY205C F_1 at 26 nM. (△): 9, wild-type F_oF_1; 10, wild-type F_1 at 26 nM; 11, wild-type F_1 at 0.5 nM plus 20 nM ϵ subunit; 12, γM23K F_oF_1; 13, γE208K F_oF_1. Lines are linear regression fits: the upper line was fit to points 1−7 ($r = 0.981$), and the lower line was fit to all other points ($r = 0.976$).

broken or made in order to achieve the transition state. This isokinetic correlation shown in Figure 4A verifies the relationship described above.

Significantly, enzymes without the ϵ subunit, carrying the γY205C substitution in F_oF_1, or F_oF_1 and F_1 enzymes in the presence of high concentrations of LDAO fall on a distinctly different line for each temperature comparison (points 1−7 in Figure 4B; for clarity, only one temperature comparison, 20 versus 35 °C, is shown). These points conform to a new linear relationship with an excellent linear regression fit (r value for the linear regression is 0.976). This includes the LDAO-treated γM23K and γE208K mutant enzymes. The enzymes treated with 10 mM LDAO fell on the same line as the enzymes depleted of ϵ subunit, indicating that LDAO disabled the ϵ subunit influence on the transition state. We emphasize that the ϵ-containing enzymes or those not treated with LDAO fell on the original line (△). Interestingly, the γY205C F_1 enzyme fell closer to the ϵ-replete line (point 8). This is likely due to a specific characteristic of this mutant enzyme or because of instability. In fact, because of instability, the temperature dependence of the ϵ-depleted γY205C enzyme could not be determined.

Table 2: Activation Energies, E_A, at 30 °C of Wild-Type Enzymes in LDAO Derived from the Arrhenius Plots Described in Figure 3

preparation	activation energy, E_A (kJ/mol)
F_oF_1 in membranes	45.8
F_oF_1 plus 10 mM LDAO	42.8
F_1 (26 nM)	59.3
F_1 (0.5 nM)	98.6
F_1 (0.5 nM) plus 20 nM ϵ subunit	47.7
F_1 (26 nM) plus 10 mM LDAO	75.5

To confirm that the effect on the thermodynamic parameters was due to the ϵ subunit, we were able to reverse the effect by adding ϵ subunit back. When wild-type F_1 was diluted below the K_D for ϵ to 0.5 nM and excess ϵ subunit was added to 20 nM, the activation energy was similar to that for the $F_1 + \epsilon$ enzyme (Figure 3 and Table 2) and the temperature dependence returned to the regression line for ϵ-replete enzymes (Figure 4, △, point 11).

DISCUSSION

In the results presented in this paper, we show that the ϵ subunit and F_o sector have control on the catalytic mechanism. The influence of the F_o sector was an approximately 2-fold activation of hydrolytic turnover over that of F_1 alone. The k_{cat} of the F_oF_1 complex uncoupled and activated by LDAO exceeded that of the $\alpha_3\beta_3\gamma$ catalytic domain complex and gave the highest k_{cat} for ATP hydrolysis obtained (890 s^{-1} at 30 °C; Figure 1A). This may be an effect of interactions with the c subunit interface because amino acid substitutions at the γ−c interface, such as γY205C, γY207C, and γE208K (*44*, *46*, *48*), affect catalytic turnover. The activation by F_o does not appear to alter the rate-limiting transition-state structure because F_1 and F_oF_1 enzymes conform to the same isokinetic relationship. Furthermore, catalysis inhibited by the transport mutant aG213N+aL251V or by venturicidin also falls on the original isokinetic relationship; therefore, attenuation by transport does not alter the transition-state structure either (*36*).

In contrast, the influence of the ϵ subunit is to decrease hydrolytic turnover of F_1 and F_oF_1. The inhibitory effect of ϵ subunit on catalysis was alleviated by LDAO or by the γY205C substitution. In agreement with previous studies (*53*, *54*), LDAO was found to activate hydrolytic turnover at concentrations of LDAO greater than 1 mM. In addition, LDAO has other effects: 0.5 mM LDAO activates hydrolytic turnover of the $\alpha_3\beta_3\gamma$ complex, and less than 0.4 mM LDAO uncouples and inhibits membranous F_oF_1. The latter effects appear to be due to disruption of the F_o structure. The characteristics of γY205C mutant enzymes were consistent with abrogation of ϵ subunit inhibition: (1) F_oF_1 and F_1 enzymes had higher hydrolytic turnover, (2) the turnover of F_1 did not increase when ϵ subunit was dissociated by dilution, and (3) the dependency on LDAO of the γY205C F_oF_1 and F_1 turnover (with bound ϵ) was very similar to that of wild-type F_1 without ϵ (Figure 1B and Table 1).

Most importantly, whereas association with the F_o sector does not alter the structure of the rate-limiting transition state of the catalytic reaction, release of ϵ inhibition does. As shown in Figure 4B, the enzymes free of the ϵ subunit, treated with 10 mM LDAO, or carrying the γY205C

mutation fell on different isokinetic lines. The isokinetic temperature, β, calculated for this line is 48 °C versus 87 °C for enzymes under the influence of the ϵ subunit (*14*). The β value may indicate the temperature of reversibility but its physical significance is debatable (*72*). Nevertheless, the excellent fits to the two different isokinetic lines combined with the consistent correlation with the release of ϵ subunit inhibition give a strong indication that the transition-state structure is different. We propose that the ϵ-subunit inhibition of catalytic turnover is a manifestation of the different transition-state structure.

Another property that correlates with ϵ-subunit inhibition and the different transition-state structure is coupling efficiency. The role of the ϵ subunit in coupling is difficult to assess because low concentrations of LDAO uncouple the transporter (Figure 2) and the *E. coli* F_1 sector will not associate with F_o in the absence of ϵ (*49*). Fortunately, the γY205C mutant enzyme provides a system for assessing the role of the ϵ subunit in coupling. The γY205C substitution causes reduced k_{cat} for ATP synthesis while the k_{cat} for ATP hydrolysis is increased, which together indicate lower coupling efficiency (Table 1). We suggest that the proper transition state structure, and therefore ϵ inhibition, is a critical feature of efficient coupling.

The partial X-ray structure of the yeast mitochondrial F_oF_1 complex shows that the mitochondrial δ subunit (equivalent of *E. coli* ϵ) interacts with the γ and c subunits and is not in physical contact with the β subunits. Several residues in the ϵ-subunit amino-terminal β-sandwich region that are involved in the interactions with the γ subunit have been identified (*39*, *43*, *44*, *73*). The lack of ϵ inhibition in the γY205C mutant enzyme, an amino acid substitution in the $\gamma-\epsilon-$c interface, suggests that the influence of ϵ subunit is mostly through its interactions with the γ subunit. Furthermore, the ϵ-subunit carboxyl-terminal region can be deleted and the enzyme complex retains active transport function (*67*, *74*). However, other results suggest that direct interactions between the ϵ carboxyl-terminal region and the α and β subunits may also have a role in ϵ inhibition and coupling efficiency. Cross-linking studies have demonstrated that the carboxyl-terminal region of the ϵ subunit contacts the α and β subunits during the course of steady-state activity (*16*, *43*, *52*, *75*−*77*). Moreover, Kato-Yamada et al. (*67*) showed that the *Bacillus* PS3 F_oF_1 with a carboxyl-terminal truncated ϵ subunit behaved like the γY205C mutant in that it had higher ATPase activity. An interesting question is whether this enzyme will also fall on the new isokinetic line.

The influence of the transport mechanism on catalysis is also through the γ subunit. The ϵ subunit and F_o have been shown to influence catalysis indirectly via conformational effects on the γ subunit (*37*, *73*, *78*). In turn, the γ subunit influences catalysis through its intimate interactions with the catalytic β subunits (*14*, *31*−*33*, *62*). Such effects were observed in the γE208K mutant (*46*) and indicated by changes in the reactivity of γY205C with maleimides that were dependent on the nucleotides and the presence of the ϵ subunit (*44*). The dynamic conformation in the interface among the γ, ϵ, and c subunits may be a part of the proposed elastic strain in the rotor, which is believed to be necessary to store energy from the multiple rotation steps produced by the transport mechanism that occur for each 120° catalytic rotation (*9*, *13*, *79*). We suggest that the conformational effects play an important role in determining the proper coupled kinetic pathway during active transport. These factors are essential not only for the transmission and conversion of energy from the transport mechanism to that of catalysis but also for its exquisite efficiency.

ACKNOWLEDGMENT

We thank Dr. Marwan Al-Shawi for help with the thermodynamic analyses and for many useful discussions.

REFERENCES

1. Duncan, T. M., Bulygin, V. V., Zhou, Y., Hutcheon, M. L., and Cross, R. L. (1995) *Proc. Natl. Acad. Sci. U.S.A. 92*, 10964−10968.
2. Sabbert, D., Engelbrecht, S., and Junge, W. (1996) *Nature 381*, 623−625.
3. Noji, H., Yasuda, R., Yoshida, M., and Kinosita, K. (1997) *Nature 386*, 299−302.
4. Aggeler, R., Ogilvie, I., and Capaldi, R. A. (1997) *J. Biol. Chem. 272*, 19621−19624.
5. Kato-Yamada, Y., Noji, H., Yasuda, R., Kinosita, K., and Yoshida, M. (1998) *J. Biol. Chem. 273*, 19375−19377.
6. Bulygin, V. V., Duncan, T. M., and Cross, R. L. (1998) *J. Biol. Chem. 273*, 31765−31769.
7. Sambongi, Y., Iko, Y., Tanabe, M., Omote, H., Iwamoto-Kihara, A., Ueda, I., Yanagida, T., Wada, Y., and Futai, M. (1999) *Science 286*, 1722−1724.
8. Pänke, O., Gumbiowski, K., Junge, W., and Engelbrecht, S. (2000) *FEBS Lett. 472*, 34−38.
9. Junge, W., Lill, H., and Engelbrecht, S. (1997) *Trends Biochem. Sci. 263*, 420−423.
10. Wang, H., and Oster, G. (1998) *Nature 396*, 279−282.
11. Fillingame, R. H., Jones, P. C., Jiang, W., Valiyaveetil, F. I., and Dmitriev, O. Y. (1998) *Biochim. Biophys. Acta 1365*, 135−142.
12. Stock, D., Leslie, A. G. W., and Walker, J. E. (1999) *Science 286*, 1700−1705.
13. Nakamoto, R. K., Ketchum, C. J., and Al-Shawi, M. K. (1999) *Annu. Rev. Biophys. Biomol. Struct. 28*, 205−234.
14. Al-Shawi, M. K., Ketchum, C. J., and Nakamoto, R. K. (1997) *Biochemistry 36*, 12961−12969.
15. Yasuda, R., Noji, H., Kinosita, K., and Yoshida, M. (1998) *Cell 93*, 1117−1124.
16. Aggeler, R., and Capaldi, R. A. (1996) *J. Biol. Chem. 271*, 13888−13891.
17. García, J. J., and Capaldi, R. A. (1998) *J. Biol. Chem. 273*, 15940−15945.
18. Vik, S. B., and Antonio, B. J. (1994) *J. Biol. Chem. 269*, 30364−30369.
19. Elston, T., Wang, H., and Oster, G. (1998) *Nature 391*, 510−513.
20. Kaim, G., Matthey, U., and Dimroth, P. (1998) *EMBO J. 17*, 688−695.
21. Zhou, Y., Duncan, T. M., and Cross, R. L. (1997) *Proc. Natl. Acad. Sci. U.S.A. 94*, 10583−10587.
22. Sorgen, P. L., Bubb, M. R., McCormick, K. A., Edison, A. S., and Cain, B. D. (1998) *Biochemistry 37*, 923−932.
23. Dunn, S. D., and Chandler, J. (1998) *J. Biol. Chem. 273*, 8646−8651.
24. McLachlin, D. T., Bestard, J. A., and Dunn, S. D. (1998) *J. Biol. Chem. 273*, 15162−15168.
25. Wilkens, S., Dunn, S. D., Chandler, J., Dahlquist, F. W., and Capaldi, R. A. (1997) *Nat. Struct. Biol. 4*, 198−201.
26. Sawada, K., Kuroda, N., Watanabe, H., Moritani-Otsuka, C., and Kanazawa, H. (1997) *J. Biol. Chem. 272*, 30047−30053.
27. Ogilvie, I., Aggeler, R., and Capaldi, R. A. (1997) *J. Biol. Chem. 272*, 16652−16656.
28. Rodgers, A. J. W., Wilkens, S., Aggeler, R., Morris, M. B., Howitt, S. M., and Capaldi, R. A. (1997) *J. Biol. Chem. 272*, 31058−31064.

29. Wilkens, S., and Capaldi, R. A. (1998) *Biochim. Biophys. Acta 1365*, 93−97.
30. Nakamoto, R. K., Maeda, M., and Futai, M. (1993) *J. Biol. Chem. 268*, 867−872.
31. Al-Shawi, M. K., Ketchum, C. J., and Nakamoto, R. K. (1997) *J. Biol. Chem. 272*, 2300−2306.
32. Al-Shawi, M. K., and Nakamoto, R. K. (1997) *Biochemistry 36*, 12954−12960.
33. Ketchum, C. J., Al-Shawi, M. K., and Nakamoto, R. K. (1998) *Biochem. J. 330*, 707−712.
34. Fraga, D., Hermolin, J., and Fillingame, R. H. (1994) *J. Biol. Chem. 269*, 2562−2567.
35. Jiang, W., and Fillingame, R. H. (1998) *J. Biol. Chem. 95*, 6607−6612.
36. Kuo, P. H., and Nakamoto, R. K. (2000) *Biochem. J. 347*, 797−805.
37. Dunn, S. D. (1982) *J. Biol. Chem. 257*, 7354−7359.
38. Soteropoulos, P., Suss, K.-H., and McCarty, R. E. (1992) *J. Biol. Chem. 267*, 10348−10354.
39. Skakoon, E. N., and Dunn, S. D. (1993) *Arch. Biochem. Biophys. 302*, 272−278.
40. Zhang, Y., Oldenburg, M., and Fillingame, R. H. (1994) *J. Biol. Chem. 269*, 10221−10224.
41. Watts, S. D., Zhang, Y., Fillingame, R. H., and Capaldi, R. A. (1995) *FEBS Lett. 368*, 235−238.
42. Zhang, Y., and Fillingame, R. H. (1995) *J. Biol. Chem. 270*, 24609−24614.
43. Tang, C., and Capaldi, R. A. (1996) *J. Biol. Chem. 271*, 3018−3024.
44. Watts, S. D., Tang, C., and Capaldi, R. A. (1996) *J. Biol. Chem. 271*, 28341−28347.
45. Watts, S. D., and Capaldi, R. A. (1997) *J. Biol. Chem. 272*, 15065−15068.
46. Ketchum, C. J., and Nakamoto, R. K. (1998) *J. Biol. Chem. 273*, 22292−22297.
47. Hermolin, J., Dmitriev, O. Y., Zhang, Y., and Fillingame, R. H. (1999) *J. Biol. Chem. 274*, 17011−17016.
48. Schulenberg, B., Aggeler, R., Murray, J., and Capaldi, R. A. (1999) *J. Biol. Chem. 274*, 34233−34237.
49. Smith, J. B., Sternweis, P. C., and Heppel, L. A. (1975) *J. Supramol. Struct. 3*, 248−255.
50. Dunn, S. D., Zadorozny, V. D., Tozer, R. G., and Orr, L. E. (1987) *Biochemistry 26*, 4488−4493.
51. Tozer, R. G., and Dunn, S. D. (1987) *J. Biol. Chem. 262*, 10706−10711.
52. Aggeler, R., Haughton, M. A., and Capaldi, R. A. (1995) *J. Biol. Chem. 270*, 9185−9191.
53. Lötscher, H.-R., deJong, C., and Capaldi, R. A. (1984) *Biochemistry 23*, 4140−4143.
54. Dunn, S. D., Tozer, R. G., and Zadorozny, V. D. (1990) *Biochemistry 29*, 4335−4340.
55. Kuo, P. H., Ketchum, C. J., and Nakamoto, R. K. (1998) *FEBS Lett. 426*, 217−220.
56. Klionsky, D. J., Brusilow, W. S. A., and Simoni, R. D. (1984) *J. Bacteriol. 160*, 1055−1060.
57. Mullis, K. B., Ferré, F., and Gibbs, R. A. (1994) *The Polymerase Chain Reaction*, Birkhäuser, Boston.
58. Sambrook, J., Fritsch, E. F., and Maniatis, T. (1989) *Molecular Cloning: A Laboratory Manual*, 2nd ed.; Cold Spring Harbor Laboratory Press, Cold Spring Harbor, NY.
59. Futai, M., Sternweis, P. C., and Heppel, L. A. (1974) *Proc. Natl. Acad. Sci. U.S.A. 71*, 2725−2729.
60. Lowry, O. H., Rosebrough, N. J., Farr, A. C., and Randall, R. J. (1951) *J. Biol. Chem. 193*, 265−275.
61. Smith, J. B., and Sternweis, P. C. (1977) *Biochemistry 16*, 306−311.
62. Nakamoto, R. K., Al-Shawi, M. K., and Futai, M. (1995) *J. Biol. Chem. 270*, 14042−14046.
63. Taussky, H. H., and Shorr, E. (1953) *J. Biol. Chem. 202*, 675−685.
64. Fabiato, A., and Fabiato, F. (1979) *J. Physiol. (Paris) 75*, 463−505.
65. Hyndman, D. J., Milgrom, T. M., Bramhall, E. A., and Cross, R. L. (1994) *J. Biol. Chem. 269*, 28871−28877.
66. Schulenberg, B., and Capaldi, R. A. (1999) *J. Biol. Chem. 274*, 28351−28355.
67. Kato-Yamada, Y., Bald, D., Koike, M., Motohashi, K., Hisabori, T., and Yoshida, M. (1999) *J. Biol. Chem. 274*, 33991−33994.
68. Sternweis, P. C., and Smith, J. B. (1980) *Biochemistry 19*, 526−531.
69. Perlin, D. S., Latchney, L. R., and Senior, A. E. (1985) *Biochim. Biophys. Acta 807*, 238−244.
70. Matsuno-Yagi, A., and Hatefi, Y. (1993) *J. Biol. Chem. 268*, 6168−6173.
71. Hausrath, A. C., Grüber, G., Matthews, B. W., and Capaldi, R. A. (1999) *Proc. Natl. Acad. Sci. U.S.A. 96*, 13697−13702.
72. Exner, O. (1973) *Prog. Phys. Org. Chem. 10*, 411−482.
73. Xiong, H., Zhang, D., and Vik, S. B. (1998) *Biochemistry 37*, 16423−16429.
74. Kuki, M., Noumi, T., Maeda, M., Amemura, A., and Futai, M. (1988) *J. Biol. Chem. 263*, 17437−17442.
75. Lötscher, H.-R., deJong, C., and Capaldi, R. A. (1984) *Biochemistry 23*, 4134−4140.
76. Dallmann, H. G., Flynn, T. G., and Dunn, S. D. (1992) *J. Biol. Chem. 267*, 18953−18960.
77. Wilkens, S., and Capaldi, R. A. (1998) *J. Biol. Chem. 273*, 26645−26651.
78. Cruz, J. A., Harfe, B., Radkowski, C. A., Dann, M. S., and McCarty, R. E. (1995) *Plant Physiol. 109*, 1379−1388.
79. Cherepanov, D. A., Mulkidjanian, A. Y., and Junge, W. (1999) *FEBS Lett. 449*, 1−6.
80. Al-Shawi, M. K., and Senior, A. E. (1988) *J. Biol. Chem. 263*, 19640−19648.

BI0013694